Emission characteristics and dynamics of species in a TEA-CO_2 laser-produced CaO plasma

J. J. CAMACHO[1] and L. DIAZ[2] E-mails: j.j.camacho@uam.es; luis.diaz@csic.es

(1) Dpto. Química-Física Aplicada, Facultad de Ciencias, Universidad Autónoma de Madrid. Cantoblanco. 28049-Madrid, Spain.

(2) Instituto de Estructura de la Materia. CFMAC. CSIC, Serrano 121, 28006-Madrid, Spain.

ABSTRACT

Laser-produced plasmas (LPPs) are nowadays a topic of great interest in fundamental and applied areas of Physics such as the manufacture of thin films by pulsed laser deposition, spectrochemical analysis through laser-induced breakdown spectroscopy (LIBS) [1-3], production of nanoparticles, etc. Laser-target interaction involves complex processes and the analysis of LPPs can be very difficult considering its transient nature as well as large variations in plasma properties with space and time. In this work, we investigated the optical emission and imaging features of plasmas produced by a high-power laser [transversely excited atmospheric (TEA) CO_2 and Nd: YAG] pulses on calcium oxide, CaO (**Fig. 1**). The analyzed plasma emission shows electronically excited neutral Ca and O atoms, ionized Ca^+, Ca^{2+}, O^+, O^{2+} and O^{3+} species and molecular bands of CaOH ($A^2\Pi$-$X^2\Sigma^+$, $B^2\Sigma^+$-$X^2\Sigma^+$ and $D^2\Sigma^+$- $A^2\Pi$) (**Fig. 2**). We focus our attention on the dynamics of the CaO LPP species expanding into vacuum. In conventional one dimensional optical emission spectroscopy (OES) studies (**Fig. 3**), various plasma-plume segments were selected along the plume expansion axis and averaged over line-of-sight. The temporal evolution of spectral atomic and ionic line intensities at a constant distance from the target has been used to build optical time-of-flight profiles (TOF) (Fig. 4a). The velocity distributions that are derived from these TOF distributions are shown in Fig. 4b. Fig. 5 gives the time evolution of electron density and its first derivative with respect to time by setting the gate width of the intensifier at 0.1 µs. This setup was easily transformed to a two-dimensional (2D) OES setup by inserting a Dove prism between the focusing and collimating lenses (Fig. 1). Time and space-resolved 2D OES plasma profiles (Figs. 6 and 7) were recorded as a function of emitted wavelength and distance from the target. Fast side-on views of the plume expansion were made by recording overall visible emission from the plasma (Fig. 8). Emission intensities of axial area at 0.1 Pa as a function of the delay are given in **Fig. 9a**. The dynamic of the plume front was compared with the shock wave expansion model (Fig. 9b).

EXPERIMENTAL

- The schematic of the setup is given in **Fig. 1**. The experiments were carried out with two nanosecond lasers (transverse excitation atmospheric CO_2, Lumonics model K-103; λ=10.591 µm) and (Nd: YAG, Litron model LPY 707G-10; λ=1.064 µm)
- The laser pulse was focused by different lenses onto the surface of CaO target at vacuum (typically at 0.1 Pa).
- Light emitted from the laser-induced plasma plume was optically imaged 1:0.5 onto the entrance slit of different spectrometers. The spectra were recorded by a gateable ICCD (Andor iStar DH-734, 1,024 × 1,024 pixels, 13 µm pixels).
- The spectra were taken at a typical distance (z) of 5 mm from the target surface.
- The delay time t_d between the laser pulse and the activation of the ICCD detector and the time interval during which the plasma emission is monitored (gate width time t_w) were adjusted by the digital delay generator of the ICCD detector.
- For recording 2D spectral images, a Dove prism inserted between two lenses was introduced into the observation optical path for rotating the plasma image by 90º. The 2D imaging studies were performed by operating the ICCD in imaging mode.

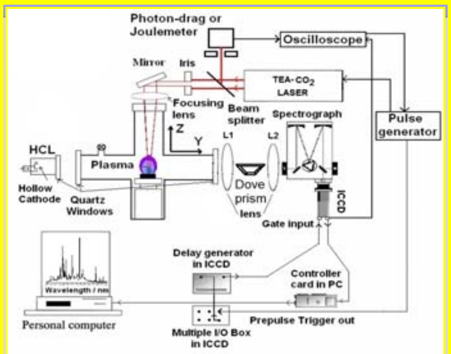

RESULTS AND DISCUSSION

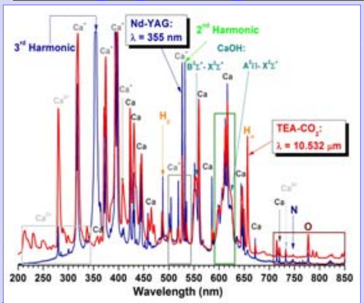

Fig. 2.-Typical LIBS emission spectra of CaO induced by a TEA-CO_2 laser (10.532 µm, 700 mJ) and a Nd:YAG laser (355 nm, 170 mJ) and assignment of Ca, Ca^+, Ca^{2+}, O, O^+, H and molecular bands of CaOH.

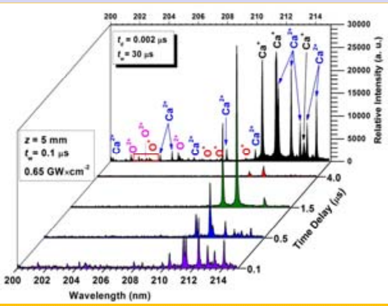

Fig. 3.- Time-resolved spectra from laser-induced (0.65 GW×cm^{-2}, P_{air}=0.1 Pa) CaO plasma at different delay times (t_w = 0.1 µs) for z=5 mm and integrated spectrum (t_w = 30 µs).

$$k_{rec} = 9.2\times10^{-27} Z^3 \ln\sqrt{Z^2+1}\cdot T_e^{-9/2}$$

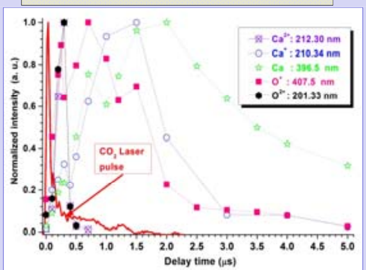

Fig. 4a.- Normalized optical TOF distributions of some Ca, Ca^+, Ca^{2+}, O^+, and O^{2+} lines as a function of delay (fixed gate width time of 0.1 µs) for a laser intensity of 0.65 GW×cm^{-2} (P_{air}=0.1 Pa) and z = 5 mm.

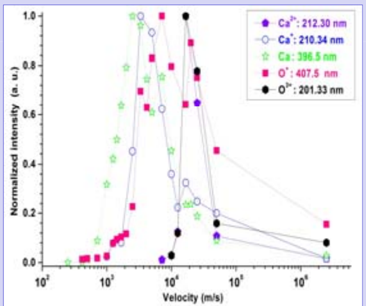

Fig. 4b.- Velocity distributions derived from the experimental TOF for the indicated species.

$$\frac{dn_e}{dt} = k_{ion} n_e N_i - k_{rec} n_e^2 N_i \approx k_{ion} n_e N_i - k_{rec} n_e^3$$

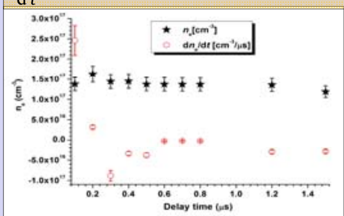

Fig. 5.-Temporal evolution of electron density n_e and first derivative dn_e/dt from conventional 1D OES (Ca II 219.7 nm, 0.65 GW×cm^{-2}, P_{air}=0.1 Pa) CaO plasma at a fixed gate width time of 0.1 µs and for z=5 mm.

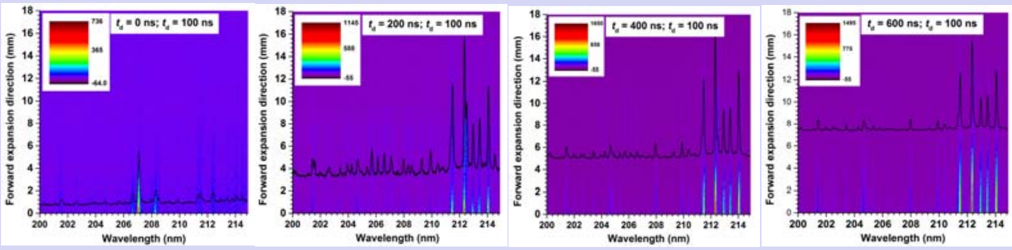

Fig. 7.-Axial space-resolved images of CaO plasma (3 GW×cm^{-2}) at delays of 0, 200, 400, 600 ns. The corresponding spectra at 1 mm are also shown.

$$\Delta\lambda^S_{FWHM} = 2W\left(\frac{n_e}{n_e^{ref}}\right) + 3.5A\left(\frac{n_e}{n_e^{ref}}\right)^{1/4}(1 - BN_D^{-1/3})W\left(\frac{n_e}{n_e^{ref}}\right)$$

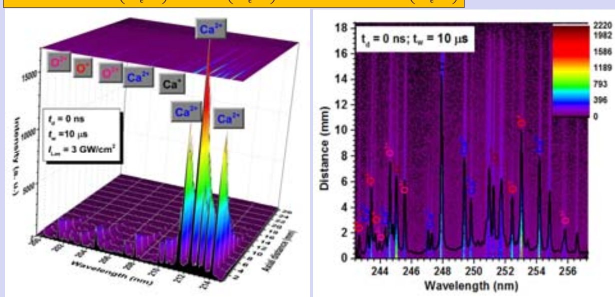

Fig. 6.-Typical axial space-resolved images in two spectral regions (3 GW×cm^{-2}, P_{air}=0.1 Pa) at a delay of 0 ns and gate width time of 10 µs. The spetra are also shown.

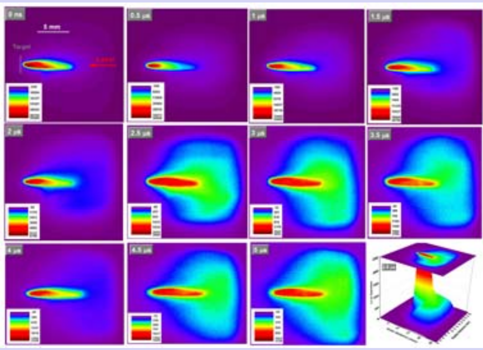

Fig. 8.-Time-resolved ICCD images of CaO at 0.1 Pa; The exposure time was t_w = 100 ns. The timings in the images represent the time after the beginning of the laser pulse. All of the images are normalized to their maximum intensity being the pseudo-color scale indicated for each figure. A 3D image at 2.5 µs is shown.

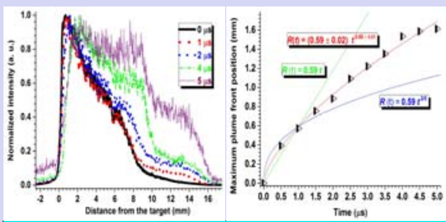

$$R = \xi_0\left(\frac{E_0}{\rho_b}\right)^{1/(n+2)} t^{2/(n+2)}$$

Fig. 9.-Normalized axial intensity profiles from the ICCD images of the plasma in vacuum (P_{air} = 0.1 Pa) as a function of time delay and distance-time (R-t) plot obtained from the ICCD images along with the fit to a shock wave model.

ACKNOWLEDGMENTS

We gratefully acknowledge the support received in part by the project MICINN (Spain) CTQ2013-43086 for this research..

[1] *J.J. Camacho, L. Diaz, M. Santos, D. Reyman, J.M.L. Poyato, J. Phys. D: Appl. Phys. 41 (2008) 105201; [2] J.J. Camacho, L. Diaz, M. Santos, L.J. Juan, J.M.L. Poyato, J. Appl. Phys. 106 (2009) 0333306.; [3] J.J. Camacho, L. Diaz, J.P. Cid, J.M.L. Poyato, Spectrochim. Acta B 88 (2013) 203.;*